

Multi-stimuli responsive fluorescence switching: the reversible piezochromism and protonation effect of a divinylanthracene derivative†

Cite this: *J. Mater. Chem. C*, 2013, **1**, 7554

Yujie Dong,^a Jibo Zhang,^a Xiao Tan,^b Lijuan Wang,^a Jinlong Chen,^a Bao Li,^a Ling Ye,^a Bin Xu,^{*a} Bo Zou^b and Wenjing Tian^{*a}

A novel divinylanthracene derivative 9,10-bis((*E*)-2-(pyridin-4-yl)vinyl)anthracene (BP4VA) was synthesized and its two polymorphs with different crystal structures were obtained. The introduction of pyridine in BP4VA leads to multi-stimuli responsive fluorescence. An investigation of the photophysical and stimuli responsive luminescent properties of BP4VA, including the piezochromism and protonation effect, demonstrates that the piezochromic luminescence originates from changes in the molecular aggregation state. Additionally, protonation–deprotonation of the pyridine moieties in BP4VA has a significant effect on the frontier molecular orbitals, resulting in distinct green and red emissions under acid and base stimuli. This study on BP4VA provides a comprehensive insight into the mechanisms within this type of stimuli-responsive luminescent material, and suggests that BP4VA may be a potential candidate for applications in sensing, detection and display devices with remarkable color-changing properties.

Received 9th August 2013

Accepted 12th September 2013

DOI: 10.1039/c3tc31553c

www.rsc.org/MaterialsC

Introduction

Stimuli-responsive luminescent materials that demonstrate a switch in emission upon external stimuli are of great importance for their potential applications in the field of optoelectronics, such as in sensors, memory devices and switches.¹ Recently, the tuning and switching of organic solid-state fluorescence based on environmental factors have been intensively studied both in the field of fundamental research and potential applications.² Several organic molecules with efficient and switchable solid state fluorescence have been developed, which respond to external stimuli such as light,³ mechanical force,⁴ vapour,⁵ etc. As for fluorescent molecules in an aggregated state, the changes in fluorescence arise not only from intramolecular effects, such as the molecular configuration and extent of conjugation, but also intermolecular effects such as, for example, π – π overlap.⁶ Piezochromic luminescent materials have been obtained through the manipulation of molecular packing modes by grinding and heating treatments.⁷ Thermo- and acid-dependent luminescent materials have also been developed based on the control of their molecular

conformations or frontier molecular orbitals.⁸ Y. Wang *et al.* investigated the vapochromic and piezochromic properties of a donor–acceptor structured compound and demonstrated that the fluorescence emission could be changed from blue to orange using different stimuli.⁹ Z. G. Chi *et al.* developed a fluorescence-switching compound with aggregation-induced emission properties based on tetraphenylethene.¹⁰ However, reports on multi-stimuli responsive fluorescent materials are quite rare, owing to the lack of clear guidelines for the design of molecules that possess all of the features of different smart materials, such as piezochromism, vapochromism and thermochromism. In addition, a detailed investigation into the related origins of these properties is also required.

Recently, we reported a series of divinylanthracene derivatives with fascinating properties.¹¹ Due to their twisted conformation and multiple supramolecular interactions, these molecules possess high solid state fluorescent quantum efficiencies and special molecular aggregation states. By modifying their molecular structures, interesting phenomena have been observed, such as aggregation-induced emission, self-assembly behaviour and amplified spontaneous emission. In particular, when pyridyl groups were introduced into the molecular structure, more supramolecular interactions such as N–H hydrogen bonds were formed, resulting in different crystal polymorphs. Such polymorphs can be used to study structural changes in molecular aggregates under mechanical force, so as to reveal the intrinsic process of the piezochromic fluorescence. Additionally, the basicity of the pyridyl group also provides an ideal model to see how the fluorescent properties can be altered

^aState Key Laboratory of Supramolecular Structure and Materials, Jilin University, Qianjin street No. 2699, Changchun, China. E-mail: wjtian@jlu.edu.cn; xubin@jlu.edu.cn; Fax: +86 431 85193421

^bState Key Laboratory of Superhard Materials, Jilin University, Qianjin street No. 2699, China

† Electronic supplementary information (ESI) available: Crystal structure refinements and Fig. S1–S3 (CCDC reference numbers 943524–943525). See DOI: 10.1039/c3tc31553c

using the stimulus of protonation.¹¹ Herein, we report a combined study based on a novel derivative 9,10-bis(*E*)-2-(pyridin-4-yl)vinyl)anthracene (BP4VA), which possesses multi-stimuli responsive fluorescent properties. Two polymorphs with high fluorescence efficiencies were successfully obtained. High pressure-PL experiments confirm that the different polymorphs of BP4VA can be used to explain its piezochromic properties. Additionally, fluorescence changes based on controlling protonation–deprotonation have been investigated, which show that different acidic/basic atmospheres can induce a switch in the emission from green to red.

Experimental section

Materials

All starting materials were purchased from Acros or Aldrich Chemical Co. and used without further purification. THF was dried by distillation from sodium/benzophenone under nitrogen.

Instruments

¹H NMR spectra were obtained using a Bruker AVANCE 500 MHz spectrometer with tetramethylsilane used as an internal standard. Time of flight mass spectra were recorded using a Kratos MALDI-TOF mass spectrometer. UV-vis absorption spectra were recorded using a Shimadzu UV-3100 spectrophotometer. Photoluminescence spectra were collected with a Shimadzu RF-5301PC spectrophotometer and Maya 2000Pro optical fiber spectrophotometer. The crystalline state PL efficiencies were measured using an integrating sphere¹² (C-701, Labsphere Inc.), with a 405 nm Ocean Optics LLS-LED as the excitation source. The excitation light was introduced into the sphere through an optical fiber.

Preparation of the crystals and the emission spectroscopy measurements

Single crystal C1 was prepared by vacuum sublimation, while single crystal C2 was prepared by slowly evaporating a mixture of chloroform and petroleum ether (3 : 1) at room temperature under the rigorous exclusion of light. The emission spectra of the crystals were obtained using the following procedure: the large-scale crystal samples were stuck on to the surface of substrates using non-emissive silica grease, and then placed into the optical path of the exciting light source. Quartz cells were used to measure the solution emission spectra.

X-ray crystallography

Diffraction experiments were carried out using a Rigaku RAXIS RAPID diffractometer equipped with a graphite-monochromator (Mo K α radiation) and control software, while in RAPID AUTO mode at 293 K. Empirical absorption corrections were applied automatically. The structures were resolved with direct methods and refined by a full-matrix least-squares fit of F^2 , using SHELX v. 5.1 software.¹³ The space groups were determined from systematic absences and their correctness was confined by the successful solution and refinement of the

structures. Anisotropic thermal parameters were refined for all of the non-hydrogen atoms. The hydrogen atoms were added at the idealized positions and refined using isotropic displacement. Crystallographic data for the structures reported in this paper are given in Table S1.†

High pressure-PL experiments

Powder and crystal samples were placed in the 200 μ m diameter holes of a T301 steel gasket, which was pre-indented to a thickness of 50 μ m. A small ruby chip was inserted into the sample compartment for *in situ* pressure calibration, utilizing the R1 ruby fluorescence method. A 4 : 1 mixture of methanol and ethanol was used as a pressure-transmitting medium (PTM). The hydrostatic-pressure conditions around the powders were determined by monitoring the widths and separation of the R1 and R2 lines. Photoluminescence measurements under high pressure were performed using a QuantaMaster 40 spectrometer in reflection mode. The 405 nm line of a violet diode laser with a spot size of 20 μ m and a power of 100 mW was used as the excitation source. The diamond anvil cell (DAC) containing the sample was put under a Nikon fluorescence microscope in order to focus the laser on to the sample. Emission spectra were obtained using a monochromator equipped with a photomultiplier. All of the experiments were conducted at room temperature.¹⁴

Results and discussion

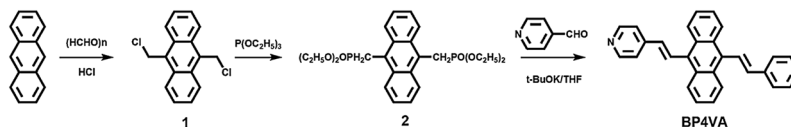
Synthesis

BP4VA was synthesized using the procedure shown in Scheme 1 and characterized by ¹H NMR, ¹³C NMR and mass spectroscopy as well as elemental analysis.

Compound **1** (9,10-bis(chloromethyl)anthracene) and compound **2** (tetraethyl anthracene-9,10-diybis(methylene) diphosphonate) were synthesized according to the previously reported methods. Compound **2** (0.500 g, 1.04 mmol) was stirred with *t*-BuOK (0.468 g, 4.17 mmol) in THF (70 mL) under nitrogen. Picolinaldehyde (0.24 mL, 2.53 mmol) in THF (70 mL) was added to the solution, which was kept in an ice-bath, and then the mixture was stirred for 12 h at room temperature. The resulting precipitate was successively washed with MeOH and then filtered off to give BP4VA as a yellow powder (50% yield).¹¹ ¹H NMR (500 MHz CDCl₃) δ 6.893–6.926 (d, J = 16.5 Hz, 2H, CH=CH), 7.514–7.534 (m, 4H, Ar), 7.544–7.556 (d, 4H, Ar), 8.153–8.186 (d, J = 16.5 Hz, 2H, CH=CH), 8.321–8.341 (m, 4H, Ar), 8.697–8.709 (d, 4H, Ar); VMALDI-TOF MS: calcd for C₂₈H₂₀N₂: 384.16, found: 383.89. Elemental anal. calcd for C₂₈H₂₀N₂: C, 87.47; H, 5.24; N, 7.29%; found: C, 86.90; H, 5.49; N, 7.21%.

Crystal structures

Single crystals with highly ordered molecular packing structures can provide direct and definitive evidence of the relationship between the molecular aggregation state and luminescence properties. By either the slow diffusion of petroleum ether vapour into a chloroform solution of BP4VA or



Scheme 1 Synthesis route of BP4VA.

vacuum sublimation, two single crystals (C1 and C2) suited for X-ray structural analysis were obtained. Through a systematic analysis of the phases of the two crystals, we found that the molecular conformations of both crystals maintained a large torsion angle (64.5° for C1 and 67.5° for C2), while the packing structures were completely different.

The unit cell of C1 is triclinic with the space group $P\bar{1}$. As shown in Fig. 1a, the main interactions between adjacent molecules in the C1 crystal were found to be CH- π interactions. In a single molecular column, a CH- π hydrogen bond (interaction 1) is formed between two molecules with an interaction distance of 2.79 Å and an angle of 145.8°, in which the pyridyl moiety along the long axis of one molecule acts as the H donor and the corresponding anthrylene core of an adjacent molecule acts as the H acceptor. For C1, the molecules adopt a stacking mode with J-type aggregation along the X axis and there is practically no overlap between the central anthracene planes, indicating that almost no π - π interactions are formed in C1.

The C2 crystals belong to the monoclinic system with the molecules adopting a stacking mode similar to H-type aggregation along the Y axis in each column. The distance between two molecules within one column in C2 is measured to be 4.02 Å, and the vertical distance between two anthracene planes is measured to be \sim 3.60 Å, as shown in Fig. 1b. Moreover, the adjacent anthracene planes overlap with each other by around 40%. In fact, there is relatively strong π - π stacking due to the large overlap between adjacent anthracene planes.¹⁵ Each molecule interacts with four neighbouring molecules *via* weak CH-N interactions (interaction 2),

which have an interaction distance and angle of 2.57 Å and 149.7°, respectively.

Photophysical properties

The UV-vis and PL spectra of BP4VA in THF solution and the PL spectra of the two single crystals are shown in Fig. 2. In THF solution, BP4VA has a main absorption peak at 410 nm and a maximum PL peak (λ_{\max}) around 584 nm. In contrast to the solution, the PL spectra of the two crystals demonstrate large blue-shifts of 52 nm (C1) and 32 nm (C2), with λ_{\max} values of around 532 nm and 552 nm, respectively. Moreover, both of the crystals exhibited quite high fluorescence quantum yields (Φ_{C1} : \sim 0.54 and Φ_{C2} : \sim 0.33), determined through integrating sphere measurements. According to our previous work, the inhibition of vibrational relaxation in the aggregation state should be the origin of the high quantum yield and blue-shift in the crystals of such a molecular system.¹¹

Additionally, the two crystals show a red-shift in their fluorescence emission and there is a decrease in the fluorescence quantum yield from C1 to C2, which could be related to the differences in their packing structures. It is worth noting that the overlap of anthracene planes between adjacent molecules is increased from C1 to C2. As described in Fig. 7a, the low-lying intramolecular electronic transition from HOMO \rightarrow LUMO in BP4VA is mainly derived from its anthracene core.¹¹ Therefore, the packing mode of the anthracene planes should play a key role in the luminescence change of the molecular aggregation state. As mentioned above, there are almost no π - π interactions in C1, while relatively strong π - π stacking exists in C2, which induces a red-shift in the PL spectrum of C2 relative to that of C1. This suggests that the PL spectrum of the aggregation state of BP4VA can be changed by adjusting its molecular packing structure.¹⁶

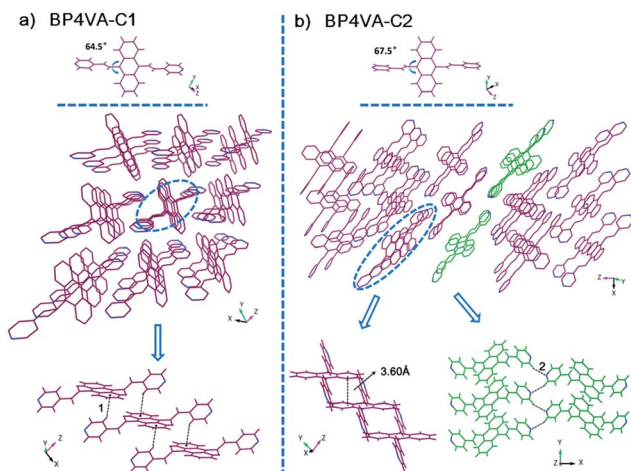


Fig. 1 The aggregation state of BP4VA in the two single crystals: (a) C1 and (b) C2.

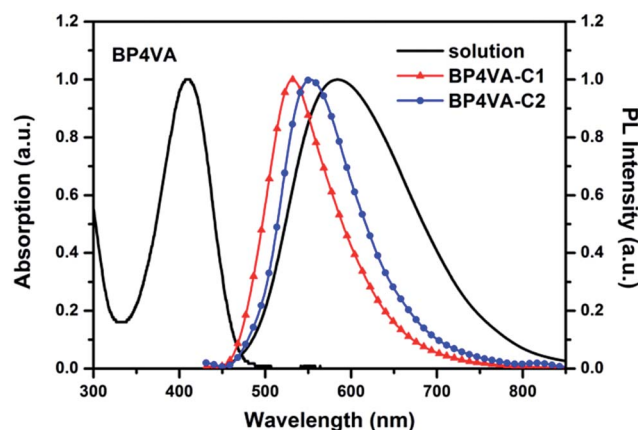


Fig. 2 Normalized absorption and PL spectra of BP4VA samples.

Piezochromic behavior

As shown in Fig. 3, the emission spectrum of the initial BP4VA powder ($\lambda_{\text{max}} \approx 523$ nm) shows green fluorescence. Once the powder has been ground using a pestle and mortar, a significant red-shift ($\lambda_{\text{max}} \approx 555$ nm) occurs and the emission band broadens. After being heated to 170 °C for about 20 min, the samples fully recover their original luminescence. This cycle can be repeated, allowing the powder to switch between the two different emission colours. In its absorption spectra, the ground powder demonstrates a weak blue-shift relative to the initial sample, suggesting that the aggregation structure changed during the grinding process (Fig. S1†).

In order to gain further insight into the origin of the fluorescence change of the BP4VA powder, powder X-ray diffraction (PXRD) experiments were conducted (Fig. 4). The diffraction pattern of the initial powder exhibits sharp and intense reflections that are consistent with the simulated XRD pattern from the crystal data of C1, suggesting that the initial sample adopts the same molecular arrangement as that of the C1 polymorph with J-type aggregation along the molecular long axis and effectively no π - π interactions between the central anthracene planes. Although some of the resolvable peaks of the ground sample are consistent with those of the unground sample, they are weaker in intensity and have broader peak shapes, indicating that the initial aggregation state was changed by grinding. This suggests that the crystal structure of BP4VA can be readily influenced by an external stimulus.

In order to further understand the piezochromic behavior, the effect of applied pressure on the luminescence of BP4VA was investigated. As shown in Fig. 5, as the applied pressure was increased, the fluorescence emission of the BP4VA powder demonstrated a gradual red-shift. Compared to the grinding method, the application of pressure from 0 to 6 GPa caused a

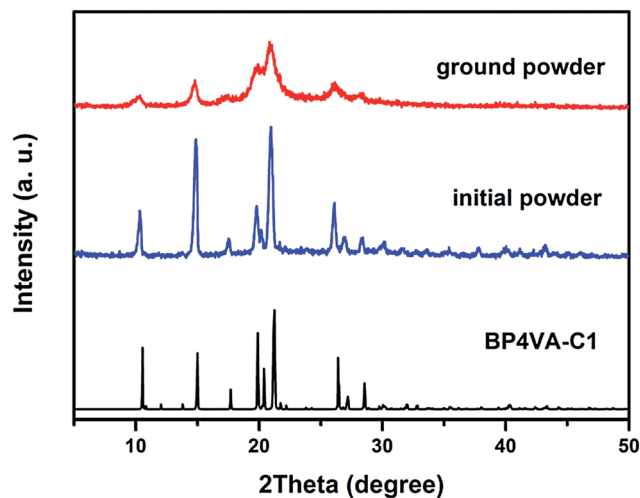


Fig. 4 The PXRD patterns of BP4VA: the ground powder, initial powder and simulated pattern obtained from the crystal data of BP4VA-C1.

more noticeable luminescence colour change of the BP4VA powder from green (523 nm) to red (650 nm). It is worth noting that the spectra exhibit multiple fluorescence peaks during the process of increasing the pressure. In particular, for the crystal sample an obvious transitional fluorescence emission can be observed, which means that it changes into a different packing polymorph as the pressure increases (Fig. S2†). Such an obvious change in the luminescent colour of the BP4VA powder and crystal samples under the applied pressure could be ascribed to changes in their molecular aggregation states under the high external pressure.^{11,16}

Protonation effect

Another notable feature of the present compound is that it shows a pronounced protonation effect. Fumigation with acid vapour has a significant effect upon the fluorescence of the BP4VA powder, turning it from green to red, while using a volatile base can lead to partial recovery of the original emission. The PL spectrum of the BP4VA powder, shown in Fig. 6,

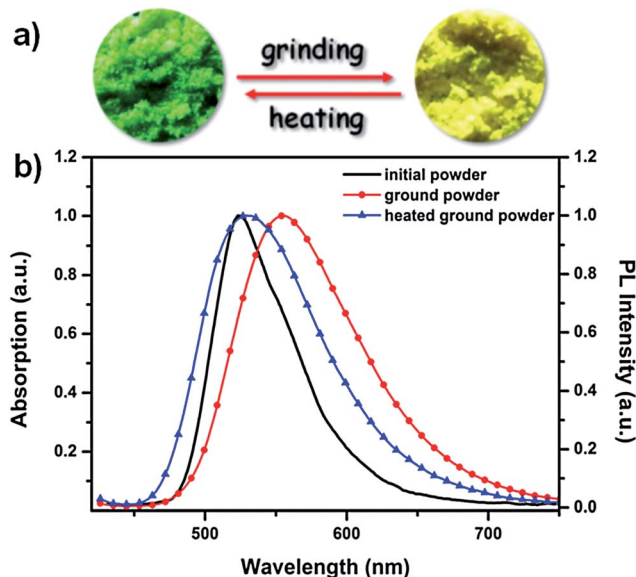


Fig. 3 (a) Photographs of the ground powder and heated powder under UV light (365 nm). (b) Absorption and PL spectra of the initial and ground samples.

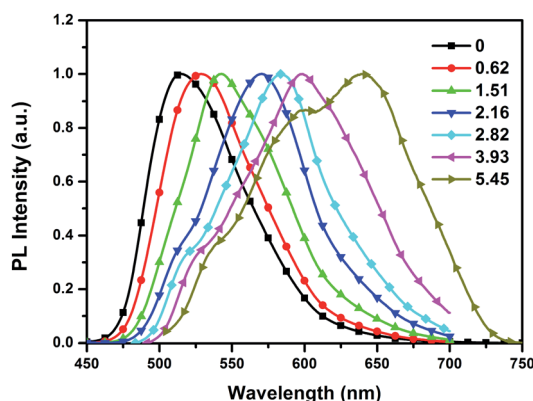


Fig. 5 Normalized solid-state PL spectra of BP4VA powder after the application of pressure (GPa).

exhibits a strong green emission peaking at 523 nm. Interestingly, after being fumed with hydrochloride (HCl) vapour, the powder gives off a red emission and the peak is shifted to 637 nm under 365 nm UV illumination. The fumed powder was also treated with alkali vapour. After being fumed with triethylamine (TEA), the original green light exhibited by the powder was recovered.

The 110 nm shift in the fluorescence and subsequent recovery towards the initial state are a demonstration of the significant fluorescence switching properties of the BP4VA powder under protonation–deprotonation stimuli. As shown in Fig. 7, when excess HCl was added into the THF solution, red-shifts were observed in both absorption (410 nm to 507 nm) and emission (584 nm to 629 nm). According to the theory of frontier molecular orbitals, for a BP4VA molecule, the Highest Occupied Molecular Orbital (HOMO) is mainly located on the divinylanthracene group, while the Lowest Unoccupied Molecular Orbital (LUMO) is partially distributed over the whole molecule. In contrast, we calculated the orbitals of the protonated BP4VA molecule, which showed that the LUMO was spread over the whole molecule with an increased electron cloud density on pyridine. Since the protonation of its nitrogen atom enhances the electron-withdrawing ability of pyridine, the LUMO should be more delocalized in the protonated molecules. Generally, the delocalization of the electron cloud is beneficial for stabilizing the molecular excited state, resulting in a decreased band gap.¹⁷ Consequently, the delocalization of the LUMO stabilizes the excited molecule at a lower band gap, leading to red-shifts in the emission and absorption of the BP4VA samples.

Considering that there is a small offset (about 8 nm) between the spectra of the HCl fumed BP4VA powder and that of BP4VA in THF/HCl solution, we think that the fluorescence switching of the fumed powder arises mostly from the change in the

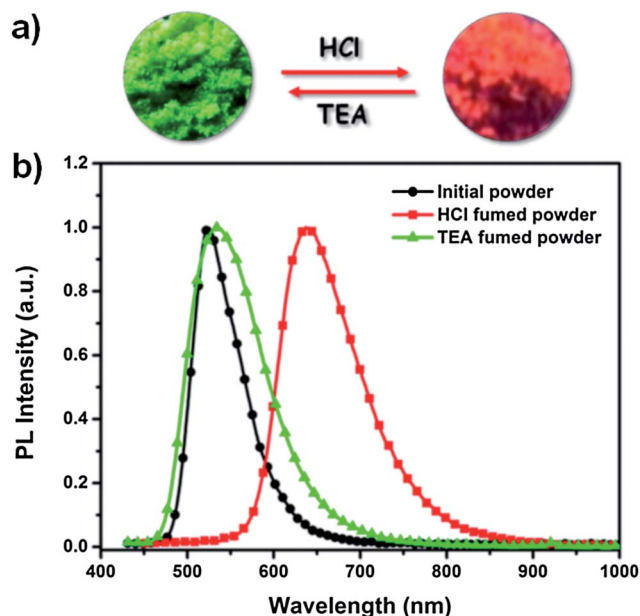


Fig. 6 (a) Photographs of the fumed powder under UV light (365 nm). (b) PL spectra of the initial, HCl fumed and TEA fumed powders.

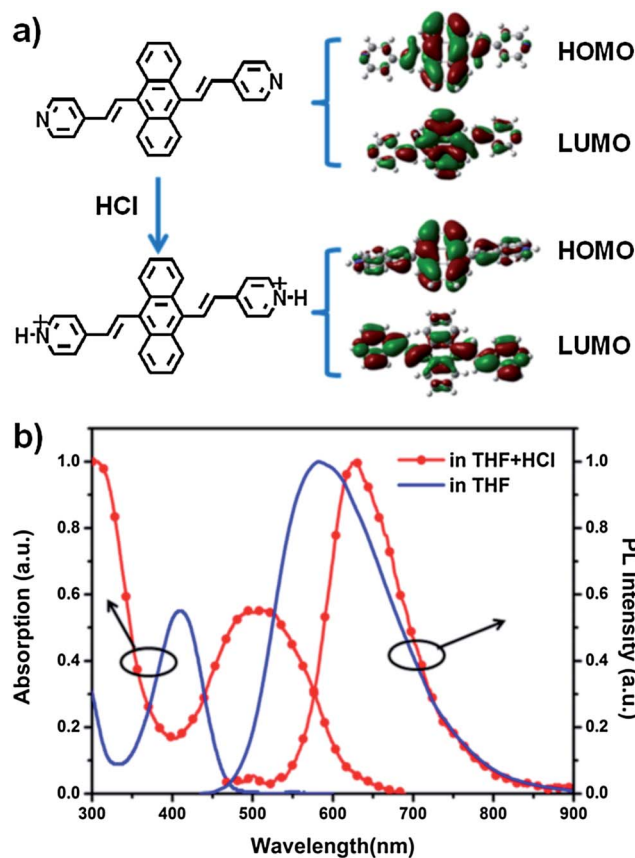


Fig. 7 (a) The molecular structures and frontier orbital contributions calculated from theory for BP4VA and its protonated form. (b) Normalized UV-vis absorption and PL spectra of BP4VA in THF and in a THF solution with excess HCl.

electron cloud density of the BP4VA molecule, which influences its frontier molecular orbitals. Meanwhile, some new supermolecular forces may be formed during this protonation process, leading to a different aggregation state and a variation in the emission.

Conclusions

We present a multi-stimuli responsive fluorescence molecule, BP4VA, which demonstrates remarkable fluorescence changes under pressure, heat, acid and base stimuli. According to the single crystal structures and high pressure PL experiments, the piezochromic behavior of the BP4VA samples originates from changes in their aggregation state under high external pressure. Photophysical and computational studies definitively confirm the protonation process of BP4VA. The protonation–deprotonation of the BP4VA powder indicates that fumigation with HCl/TEA vapour leads to a transformation of the compound's frontier molecular orbitals between its protonated and unprotonated forms, resulting in distinct green and red emissions. This study on BP4VA provides a comprehensive insight into the origins of the properties in this type of stimuli-responsive luminescent material, and suggests that it may be a potential candidate for applications in sensing, detection and display devices with remarkable color-changing properties.

Notes and references

- 1 (a) Y.-C. Chang and S.-L. Wang, *J. Am. Chem. Soc.*, 2012, **134**, 9848–9851; (b) W.-E. Lee, Y.-J. Jin, L.-S. Park and G. Kwak, *Adv. Mater.*, 2012, **24**, 5604; (c) S. Roy, S. P. Mondal, S. K. Ray and K. Biradha, *Angew. Chem., Int. Ed.*, 2012, **51**, 12012; (d) Z. Zhang, D. Yao, T. Zhou, H. Zhang and Y. Wang, *Chem. Commun.*, 2011, **47**, 7782; (e) B. Xu, Z. Chi, J. Zhang, X. Zhang, H. Li, X. Li, S. Liu, Y. Zhang and J. Xu, *Chem.-Asian J.*, 2011, **6**, 1470; (f) Z. Chi, X. Zhang, B. Xu, X. Zhou, C. Ma, Y. Zhang, S. Liu and J. Xu, *Chem. Soc. Rev.*, 2012, **41**, 3878; (g) X. Zhang, Z. Chi, Y. Zhang, S. Liu and J. Xu, *J. Mater. Chem. C*, 2013, **1**, 3376.
- 2 (a) S. J. Yoon, J. W. Chung, J. Gierschner, K. S. Kim, M. G. Choi, D. Kim and S. Y. Park, *J. Am. Chem. Soc.*, 2010, **132**, 13675; (b) S. P. Anthony, *ChemPlusChem*, 2012, **77**, 518; (c) O. Dautel, M. Robitzer, J. P. Lere-Porte, F. Serein-Spirau and J. Moreau, *J. Am. Chem. Soc.*, 2006, **128**, 16213.
- 3 J. W. Chung, Y. You, H. S. Huh, B.-K. An, S.-J. Yoon, S. H. Kim, S. W. Lee and S. Y. Park, *J. Am. Chem. Soc.*, 2009, **131**, 8163.
- 4 (a) Y. Sagara and T. Kato, *Nat. Chem.*, 2009, **1**, 605; (b) M. S. Kwon, J. Gierschner, S.-J. Yoon and S. Y. Park, *Adv. Mater.*, 2012, **24**, 5487; (c) X. Luo, J. Li, C. Li, L. Heng, Y. Q. Dong, Z. Liu, Z. Bo and B. Z. Tang, *Adv. Mater.*, 2011, **23**, 3261.
- 5 T. Zhou, T. Jia, S. Zhao, J. Guo, H. Zhang and Y. Wang, *Cryst. Growth Des.*, 2012, **12**, 179.
- 6 (a) Y. Sagara and T. Kato, *Angew. Chem., Int. Ed.*, 2008, **47**, 5175; (b) S. Yamaguchi, T. Shirasaka, S. Akiyama and K. Tamao, *J. Am. Chem. Soc.*, 2002, **124**, 8816.
- 7 (a) J. Kunzleman, M. Kinami, B. R. Crenshaw, J. D. Protasiewicz and C. Weder, *Adv. Mater.*, 2008, **20**, 119; (b) Y. Sagara, T. Mutai, I. Yoshikawa and K. Araki, *J. Am. Chem. Soc.*, 2007, **129**, 1520.
- 8 (a) Y. Zhao, H. Gao, Y. Fan, T. Zhou, Z. Su, Y. Liu and Y. Wang, *Adv. Mater.*, 2009, **21**, 3165; (b) A. Pucci and G. Ruggeri, *J. Mater. Chem.*, 2011, **21**, 8282.
- 9 C. Dou, L. Han, S. Zhao, H. Zhang and Y. Wang, *J. Phys. Chem. Lett.*, 2011, **2**, 666.
- 10 (a) B. Xu, M. Xie, J. He, B. Xu, Z. Chi, W. Tian, L. Jiang, F. Zhao, S. Liu, Y. Zhang, Z. Xu and J. Xu, *Chem. Commun.*, 2013, **49**, 273; (b) X. Zhang, M. Liu, B. Yang, X. Zhang and Y. Wei, *Colloids Surf., B*, 2013, **112**, 81; (c) B. Xu, Z. Chi, X. Zhang, H. Li, C. Chen, S. Liu, Y. Zhang and J. Xu, *Chem. Commun.*, 2011, **47**, 11080; (d) X. Zhou, H. Li, Z. Chi, X. Zhang, J. Zhang, B. Xu, Y. Zhang, S. Liu and J. Xu, *New J. Chem.*, 2012, **36**, 685.
- 11 (a) Y. Dong, B. Xu, J. Zhang, X. Tan, L. Wang, J. Chen, H. Lv, S. Wen, B. Li, L. Ye, B. Zou and W. Tian, *Angew. Chem., Int. Ed.*, 2012, **51**, 10782; (b) J. Zhang, J. Chen, B. Xu, L. Wang, S. Ma, Y. Dong, B. Li, L. Ye and W. Tian, *Chem. Commun.*, 2013, **49**, 3878; (c) Y. Dong, B. Xu, J. Zhang, H. Lu, S. Wen, F. Chen, J. He, B. Li, L. Ye and W. Tian, *CrystEngComm*, 2012, **14**, 6593.
- 12 J. C. de Mello, H. F. Wittmann and R. H. Friend, *Adv. Mater.*, 1997, **9**, 230.
- 13 SHELXTL, *Version 5.1*, Siemens Industrial Automation, Inc., 1997.
- 14 S. R. Li, Q. Li, J. Zhou, R. Wang, Z. M. Jiang, K. Wang, D. P. Xu, J. Liu, B. B. Liu, G. T. Zou and B. Zou, *J. Phys. Chem. B*, 2012, **116**, 3092.
- 15 C. A. Hunter and J. K. M. Sanders, *J. Am. Chem. Soc.*, 1990, **112**, 5525.
- 16 K. Nagura, S. Saito, H. Yusa, H. Yamawaki, H. Fujihisa, H. Sato, Y. Shimoikeda and S. Yamaguchi, *J. Am. Chem. Soc.*, 2013, **135**, 10322.
- 17 V. Bernard, *Molecular Fluorescence Principles and Applications*, Wiley-VCH, 2002, p. 54.